Stokes–anti-Stokes Brillouin intensity asymmetry of spin-wave modes in ferromagnetic films and multilayers

R. Zivieri, P. Vavassori, L. Giovannini, and F. Nizzoli
Dipartimento di Fisica, Università di Ferrara and Istituto Nazionale per la Fisica della Materia, Via Paradiso 12, I-44100 Ferrara, Italy

Eric E. Fullerton
IBM Almaden Research Center, San Jose, California 95120-6099

M. Grimsditch and V. Metlushko
Materials Science Division, Argonne National Laboratory, Argonne, Illinois 60439-4845
(Received 5 September 2001; published 4 April 2002)

The Stokes–anti-Stokes intensity asymmetry, observed in Brillouin spectra from magnetic excitations, has been investigated experimentally and theoretically in single and multilayer films. In single films our investigation has led to a simple physical picture for the origin of the Stokes–anti-Stokes asymmetry and its dependence on polarization, magnetic field, and scattering geometry. In ferromagnetic bilayers and trilayers, while the full theory is needed to produce a quantitative description of the experimental results, the simple physical picture provides a useful qualitative guide to understanding the results.

DOI: 10.1103/PhysRevB.65.165406 PACS number(s): 78.35.+c, 75.30.Ds, 75.70.−i

I. INTRODUCTION

Although the asymmetry of the Stokes (S) and anti-Stokes (AS) portions of Brillouin light scattering (BLS) from magnetic materials has received considerable attention, there are still some intriguing aspects that warrant a more careful analysis. Early experiments observed large differences in the intensity of the S and AS lines that could not be understood on the basis of thermal population levels.[1] These observations were correctly attributed to the role of time-reversal symmetry in magnetic systems. In the bulk of a ferromagnet, although the frequency ω of an excitation with wave vector $\mathbf{q}$ satisfies $\omega(\mathbf{q})=\omega(-\mathbf{q})$, time-reversal effects still produce asymmetries in the ratio of S and AS intensities due to the relative phases of the contributions to scattered light. More spectacular is the effect of time reversal on surface modes on ferromagnets where it leads to nonreciprocal behavior. Not only is $\omega(\mathbf{q})\neq\omega(-\mathbf{q})$, but one of these modes may not exist; i.e., surface magnons on a ferromagnet propagate only in one direction. The result of this is that they appear only as S or AS lines in the spectra.

When dealing with thin films the problem is complicated further by the fact that the amplitude of the surface mode on the back surface of the film now has a finite amplitude on the front surface. When this occurs, the missing S or AS line in the Brillouin spectrum becomes observable. In the limit when the film is much thinner than the wavelength of the excitations (so that the amplitudes on the front and back surfaces are essentially equal) one might expect the Stokes–anti-Stokes (S-AS) asymmetry to vanish. Experimentally, however, there is evidence that the S-AS ratio does not approach unity as the thickness is reduced. The explanation, as described in the theoretical treatments of Camley *et al.*[1,2] and Cochran and Dutcher,[3] is the relative phase of different contributions to the scattering. Since contributions to the scattering arise from different components of the dynamic magnetization vector as well as from both linear and quadratic coupling terms, it is not always straightforward to isolate the origin of the asymmetry in a particular situation. The above complexities have precluded the formulation of simple arguments that account for many of the observed phenomena: dependence of the S-AS asymmetry on applied field, scattering geometry, magnon wave vector, film thickness, and substrate material.[4,5]

The aim of this paper is to discuss the consequences of time reversal for the case of ferromagnetic films and multilayers of increasing complexity. In order to do this we first present arguments that explain in simple terms the behavior in a single ferromagnetic film. Even for this ''simple'' case, however, there are some surprises. We then focus on the field dependence of the asymmetry in Brillouin spectra from Fe/Cr multilayers with equal and unequal Fe layer thicknesses; in the latter case the loss of inversion symmetry in the geometry provides a particularly insightful description.

II. SINGLE FILM

Fe is particularly well suited to this investigation since it is known that the quadratic magneto-optical constants produce negligible contributions to the scattering.[1,6] This allows us to restrict the theoretical description to only linear terms allowing a much clearer interpretation of the role of time-reversal symmetry. In order to highlight some of the effects we choose the following scattering geometry: the film lies in the x-z plane, with the magnetic field applied along the z direction. Light of wave vector k_0 is incident in the x-y plane (incidence plane) at an angle θ from the surface normal (y) and the collection lens lies along the surface normal. The resulting magnon wave vector $\mathbf{q}$ is along the x direction and its magnitude is equal to $k_0\sin\theta$.

For an incident electric field that oscillates at a frequency ω_0 its interaction with the magnetic fluctuations of frequency ω gives rise to scattered radiation at the sum (AS) and difference (S) frequencies $\omega_0\pm\omega$, respectively.[7] Following Co-

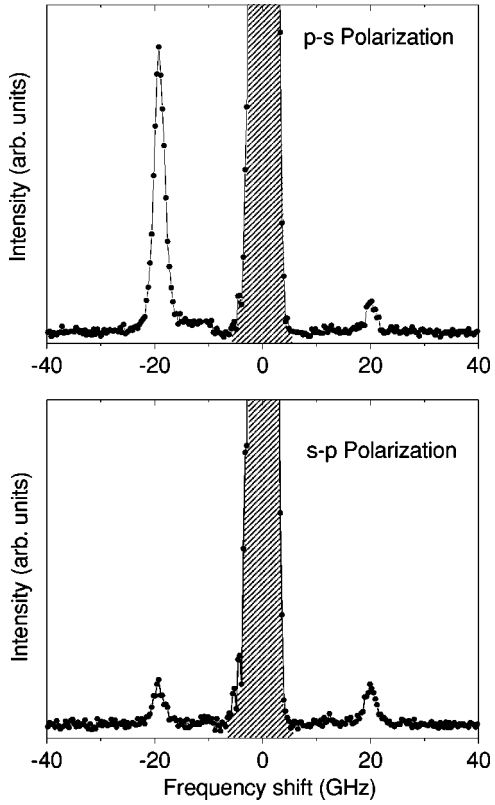

FIG. 1. BLS spectra from a 17.1-nm Fe film for $\theta=65°$ at $H=150$ Oe. (a): *p*-*s* geometry. (b): *s*-*p* geometry. The shadowed area identifies the peak due to the unshifted laser light.

chran and Dutcher[3] the intensity of these two processes depends on the scattering geometry and on the polarization of the incident light. If the incident light is polarized in the incidence plane (i.e., *p* polarized light) the intensities will be an integral of terms of the form

$$I_S \propto |(m_y E_x - m_x E_y)|^2 \quad \text{and} \quad I_{AS} \propto |(m_y^* E_x - m_x^* E_y)|^2 \quad (1)$$

for the S and AS, respectively. When the incident light is polarized along z, i.e., perpendicular to the incidence plane (viz. *s* polarized light) the intensity will depend on terms of the form

$$I_S \propto |m_y E_z|^2 \quad \text{and} \quad I_{AS} \propto |m_y^* E_z|^2. \quad (2)$$

In the previous equations m_x, m_y, E_x, E_y, and E_z are the complex amplitudes of the dynamic magnetization and the electric-field components, respectively. We stress that Eq. (2) is particularly simple only because we have chosen the scattering geometry for collection along the surface normal. In a thick opaque film, for surface magnons which are localized on the front and back surfaces, only a S or an AS peak is observed because the electric fields at the back surface are negligible. In a thin film (i.e., thickness $\gg q^{-1}$) the values of *m* for the front and back modes become essentially equal. In this limit Eq. (2) predicts no asymmetry while Eq. (1) does not preclude a possible asymmetry.

Supporting this prediction, Fig. 1 shows two spectra from an epitaxial (001) Fe film on Ge substrate recorded in tandem mode with *p*-*s* and *s*-*p* polarizations of 514.5-nm radiation at an incidence angle $\theta=65°$ and with $H=150$ Oe along the easy axis. The thickness and the magnetic parameters of our Fe film obtained from a fit to the Brillouin frequencies of the surface and standing modes with the field along the hard and easy axes are: thickness $d=17.1$ nm, saturation magnetization $4\pi M=20.3$ kG, and magnetocrystalline anisotropy constant $K_1=3.45\times10^5$ ergs/cm^3.

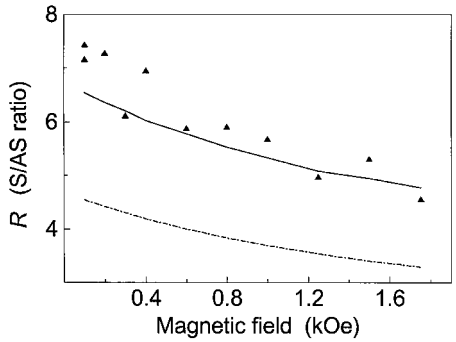

FIG. 2. S-AS intensity ratio as a function of the applied field *H*. Triangles: BLS experimental data for $\theta=45°$. Solid line: calculated results obtained with the full theory and the fitted parameters listed in the text. Dashed line: approximate calculation obtained from Eqs. (3)–(5).

As pointed out by Camley[8] the asymmetry in the spectra like the one in Fig. 1(a) is due to the relative phase of the contributions of m_x and m_y. From Eq. (1) the S-AS intensity ratio (R) can be written

$$R=\frac{|1-(m_x/m_y)(E_y/E_x)|^2}{|1-(m_x/m_y)^*(E_y/E_x)|^2}. \quad (3)$$

Note that Eq. (3) does not depend explicitly on the wave vector **q** of the magnon. However, as we will show, the ratio m_x/m_y does depend on q. Equation (3) shows that if E_y/E_x is real (i.e., the field components are in phase), there will be no asymmetry so that in a transparent ferromagnet $R=1$ is expected. In a material with a complex dielectric constant ϵ we can write

$$\frac{E_y}{E_x}=\frac{\sin\theta}{\sqrt{\epsilon-\sin^2\theta}} \quad (4)$$

In general the ellipticity of the precession, defined as the ratio $|m_x|/|m_y|$, will depend on the particular mode that is being probed and requires a complete calculation of the normal modes including anisotropies and finite thickness effects. However, for a thin film of thickness *d* the mode, with wave vector **q** probed by Brillouin scattering, is approximately described by the ferromagnetic resonance frequency with finite thickness corrections. In this case $|m_x|/|m_y|$ is given by [see Eqs. (A1) and (A2) in Ref. 9]

$$\frac{|m_x|}{|m_y|}=\frac{\sqrt{H+4\pi M-2\pi Mqd}}{\sqrt{H+2\pi Mqd}}. \quad (5)$$

In Fig. 2 we show the field dependence of the S-AS in-

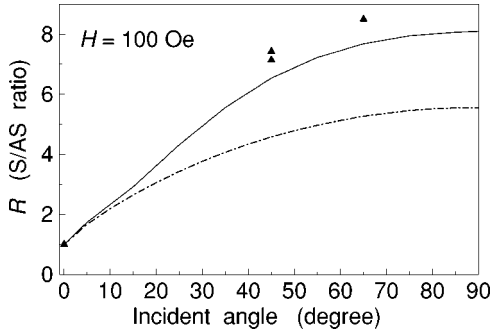

FIG. 3. S-AS intensity ratio as a function of the light incident angle. Triangles: BLS experimental data. Solid line: full calculation. Dashed line: approximate calculation obtained from Eqs. (3)–(5).

tensity ratio for the same film described in Fig. 1 but with $\theta=45°$. Triangles are experimental points and the dashed line was obtained from Eqs. (3)–(5) with $\epsilon=-0.4+16.3\,i$.[10] As predicted by Eq. (3) we observe a reduction in the intensity ratio as the field is increased and this reduction can be traced to the field induced changes in $|m_x|/|m_y|$ ratio in Eq. (5), from 3.5 to 2.5 in the range considered. The discrepancies between the experimental points and the dashed line in Fig. 2 can be traced to the approximations that have been made. Neglect of the radiation reflected at the Fe/Ge and Fe/air interfaces [viz. Eq. (4)] is the largest source of discrepancy between the dashed line and the experimental data in Fig. 2. The effect of these reflections is to change the relative phase and amplitudes of E_x and E_y in the Fe layer and explains the large changes in asymmetry reported in Ref. 5 for Fe films deposited on Au and GaAs. The neglect of anisotropy and the approximate nature of Eq. (5) (valid only for $qd\ll 1$) produce only small changes. The full theoretical calculation, that incorporates all the above contributions, and shown by the full line in Fig. 2, achieves excellent agreement with the experimental results except at low fields where the measurements are underestimated.

The S-AS ratio dependence on the angle of incidence θ contains two contributions. Changes in θ affect the E_x/E_y ratio, as shown in Eq. (4) when multiple reflections are ignored, but also affect the $|m_x|/|m_y|$ ratio via the change in magnon wave vector q in Eq. (5). In Fig. 3 we have plotted the intensity ratio as a function of θ for $H=100$ Oe. The triangles are experimental points measured at 45° and 65°. The dashed line is obtained from Eqs. (4) and (5) and the full line represents the full theoretical calculation. One notes that the S-AS calculated ratio increases monotonically with increasing the incident angle and underestimates the experimental data. Although technical problems did not allow the measurements of the ratio for $\theta<45°$, we know that the value of this ratio for $\theta\rightarrow 0$ must be equal to that measured in the *s-p* configuration (in this configuration the ratio is independent of θ), i.e., equal to 1 as indicated in Fig. 3.

III. FERROMAGNETIC BILAYER

The bilayer we will describe in this section is the (211)-Fe(20 Å)/Cr(11 Å)/Fe(20 Å) sample investigated in Ref. 9. The two 20-Å-thick Fe films in this structure are coupled antiferromagnetically (AF); at low fields the two Fe layers are aligned antiparallel and at high fields they switch to being aligned parallel to each other. Two experimental spectra recorded in the *p-s* polarization for the antialigned and aligned states are shown in Fig. 4. Note that these spectra have been recorded in five-pass mode and the assignment of the different peaks is tricky due to the presence of ghosts and instrumental artefacts (see caption of Fig. 4). In spite of the noise, it is interesting to note that, contrary to the case of a single film, these spectra do not exhibit large S-AS intensity asymmetries. The two S-AS doublets expected for this sample are labeled as modes 1 and 2. The two spectra shown on the right of Fig. 4 were obtained from a full cross-section calculation[11] using the magnetic parameters given in Ref. 9. Although the calculated spectra reproduce the measured intensity ratios they do not provide a direct and transparent explanation for the small S-AS asymmetries, because these calculations depend on many factors (film thickness, distri-

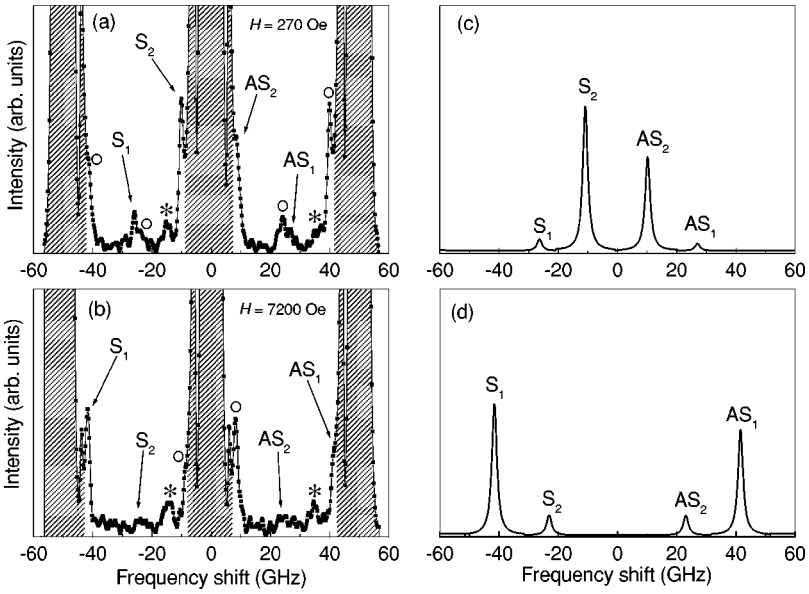

FIG. 4. Experimental BLS spectra in the *p-s* polarization [(a) and (b)] and corresponding calculated intensities [(c) and (d)] for the ferromagnetic bilayer for the antialigned and aligned states. The shadowed area identifies the peaks related to the unshifted laser light. Other instrumental artefacts are labeled by asterisks. Open circles mark the position of ghosts present in the spectra, which are collected in five-pass mode.

TABLE I. Dynamic magnetization components of film 1 and 2 at two different external fields. ω_+ represents the highest frequency mode and ω_- the lowest frequency one. The listed numerical values are normalized to unity.

	m_{x1}	m_{y1}	m_{x2}	m_{y2}
$\omega_-(H=0.27$ kOe)	0.65	$-0.11\ i$	-0.74	$-0.13\ i$
$\omega_+(H=0.27$ kOe)	0.69	$-0.34\ i$	0.57	$0.29\ i$
$\omega_-(H=7.2$ kOe)	-0.66	$0.26\ i$	0.66	$-0.25\ i$
$\omega_+(H=7.2$ kOe)	0.62	$-0.35\ i$	0.62	$-0.35\ i$

bution of the electric fields, electric-field wave vectors, magnon ellipticity, etc.).

Further insight can be gained from a generalization of Eq. (1) viz.

$$I \propto |(m_{y1}+m_{y2})E_x-(m_{x1}+m_{x2})E_y|^2 \tag{6}$$

and its equivalent for the AS case, i.e., with the complex conjugate magnetizations. The subscripts 1 and 2 refer to the two Fe films. This equation neglects possible changes in the magnitudes of E_x and E_y with depth, but should be a good approximation for the sample discussed. To use Eq. (6) it is necessary to know the relative magnitudes and phases of the dynamic magnetizations of the two layers, which can be obtained by a number of methods (see, for example, Refs. 9 and 12). For this particular sample and the applied fields of Fig. 4 the normalized magnetizations are given in Table I. Note that at high fields for ω_- there is exact cancellation of m_x in Eq. (6) leading to no asymmetry and an almost exact cancellation of m_y leading to a very weak intensity. For ω_+ mode it is the small ellipticity ($|m_x|/|m_y| \simeq 1.8$) combined with $|E_y|/|E_x| \simeq 1/8$ for this scattering geometry that leads to the small intensity asymmetry. For low fields it is either the m_x or the m_y components that almost cancel leading to only one dominant contribution in Eq. (6) and again yielding small S-AS asymmetries. To summarize: the small S-AS intensity ratio in a bilayer is due to the fact that in all cases there is a dominant term in Eq. (6). Although there is a strong variation of ellipticity with H (see Table I) its influence on the asymmetry is almost completely masked by the cancellation effects.

IV. FERROMAGNETIC TRILAYER

We conclude with a discussion of a ferromagnetic trilayer with layers of different thickness and in which both ferromagnetic (F) and AF coupling between the layers are simultaneously present. The sample we will use for this investigation is (211)-Fe(20 Å)/Cr(20 Å)/Fe(20 Å)/Cr(9 Å)/Fe(100 Å).[13] Three modes are now expected on the S and AS sides of the spectra. The frequencies and the material parameters extracted from them have been presented in Ref. 13. Here we will deal only with the intensity of the Brillouin peaks.

In Fig. 5 we show tandem mode experimental and calculated spectra for two applied fields. At the low field ($H=355$ Oe) the static magnetization of the thick film is aligned with the external field, while the static magnetizations of the other two films are both antialigned with **H**. At the high field ($H=3400$ Oe) all three layers are aligned with the applied field. In contrast to the bilayer system the spectra for the trilayer again exhibit large S-AS asymmetries which are well accounted for by the full theory, as shown in Fig. 5. Based on the different thickness of the various layers and the loss of a center of inversion, one can envision that cancellations of the magnetizations are now much less likely and that consequently large S-AS intensity asymmetries should be expected. At a qualitative level the asymmetries in Fig. 5 can also be understood by calculating the amplitude of the dynamic magnetizations for each layer: these values are shown in Table II together with the corresponding ellipticities. As can be seen in Table II, in this asymmetric heterostructure the amplitudes of the dynamic magnetization are distributed in a very different way depending on the particular mode. At both low and high fields there is a mode mainly localized in the outermost layer (acoustical according to the definition of Ref. 12) which is expected to give rise to the

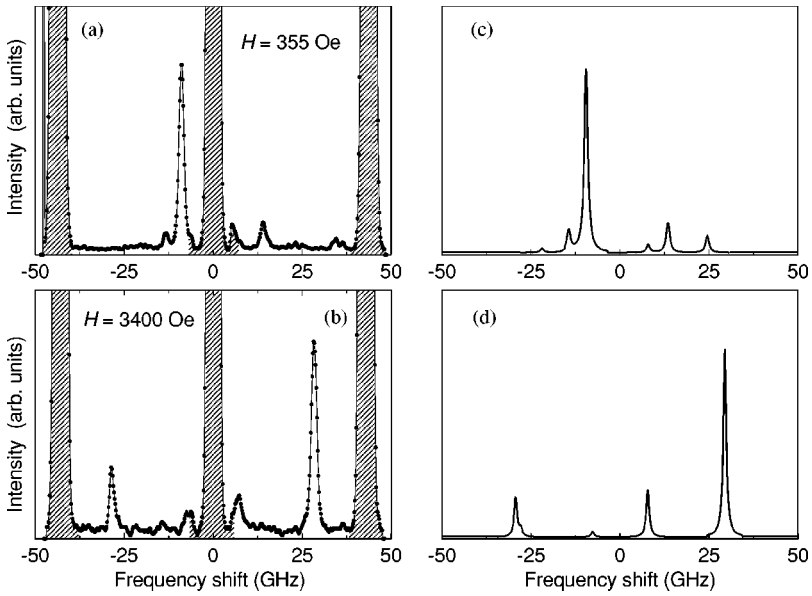

FIG. 5. Measured BLS spectra [(a) and (b)] and corresponding calculated intensities [(c) and (d)] for the ferromagnetic trilayer at two different external fields. The shadowed area identifies the peaks related to the unshifted laser light.

TABLE II. Dynamic magnetization components of film 1, 2 and 3 at two different external fields. ω_+ represents the highest frequency mode, ω_- the lowest frequency one, and ω_o the mode at intermediate frequency. The label 1 indicates the outermost layer. The listed numerical values are normalized to unity. The divergence of $|m_{x1}|/|m_{y1}|$ for ω_+ ($H=0.35$ kOe) is a numerical artefact due to the instability of the film 1 near the transition.

	m_{x1}	m_{y1}	$\lvert\frac{m_{x1}}{m_{y1}}\rvert$	m_{x2}	m_{y2}	$\lvert\frac{m_{x2}}{m_{y2}}\rvert$	m_{x3}	m_{y3}	$\lvert\frac{m_{x3}}{m_{y3}}\rvert$
$\omega_-(H=0.35$ kOe)	-0.91	$-0.17\ i$	5.4	-0.32	$-0.05\ i$	6.4	0.20	$-0.03\ i$	6.7
$\omega_o(H=0.35$ kOe)	0.60	$0.17\ i$	3.5	-0.64	$-0.16\ i$	4	0.41	$-0.11\ i$	3.7
$\omega_+(H=0.35$ kOe)	-0.07	$0\ i$		0.91	$0.36\ i$	2.5	0.19	$-0.10\ i$	1.9
$\omega_-(H=3.4$ kOe)	-0.08	$0.01\ i$	8	-0.96	$0.12\ i$	8	0.22	$-0.02\ i$	11
$\omega_o(H=3.4$ kOe)	-0.59	$0.27\ i$	2.2	0.52	$-0.25\ i$	2.1	0.45	$-0.22\ i$	2
$\omega_+(H=3.4$ kOe)	0.89	$-0.41\ i$	2.2	0.07	$-0.06\ i$	1.2	0.14	$-0.08\ i$	1.8

largest peak in the spectra due to the strong interaction with the light. This behavior is clearly exhibited by Fig. 5. The intensity of the corresponding S and AS doublets is strongly asymmetric especially at low field, where the ellipticity in the outermost layer is quite large.

Another mode (ω_+ at low field and ω_- at high field) shows from Table II a large localization in the central layer, where the light is partially attenuated, therefore the corresponding scattering intensity is weak. Again a large ellipticity (as for ω_- at high field) gives rise to a strong S-AS asymmetry. The behavior of the remaining mode (ω_o) is quite intriguing, because the uniform localized magnetization across the layers and the attenuation of light makes difficult to apply also to this case Eq. (6) in order to predict in simple way the intensity and S-AS asymmetry of the BLS doublets. As a matter of fact, the ω_o doublet at low field is rather weak and almost symmetric both in experiment and calculation, while the doublet at high field is too close to the strong feature ω_+ to draw any conclusion.

V. CONCLUSIONS

Although the S-AS intensity asymmetry observed in Brillouin spectra from ferromagnetic films is known to be a peculiarity of time-reversal symmetry, it is much less clear why it should depend on: the strength of the applied field, the scattering geometry, nature of the substrate polarization of the radiation and mode localization. Here we show how these effects can be understood on the basis of the ellipticity of the magnons and on the relative phase of the electric-field components.

In the case of a single film for *p-s* scattering geometry we have shown that the main features of the S and AS Brillouin intensities and of their ratio may be described in terms of simple approximated equations. An important role is played by the ellipticity of the spin wave which, in addition to the external field, depends on the film thickness and on the magnon wave vector. The decrease of the ellipticity with increasing external field is responsible for the behavior of the S-AS intensity ratio in qualitative agreement with the experimental data. We have also found that in order to obtain quantitative agreement a full calculation of the BLS cross section taking into account the electromagnetic boundary conditions at the film-substrate interface is necessary.

In a symmetric Fe/Cr/Fe ferromagnetic bilayer we find that cancellations of the dynamic magnetizations of the two layers lead to S-AS intensity ratios which are close to unity. The lack of cancellation between the dynamic magnetization of the various layers in an asymmetric Fe/Cr/Fe/Cr/Fe multilayer produces in general large S-AS asymmetries. In this case, the ellipticity and the localization of the dynamic magnetization control the S-AS ratio.

The analysis presented here highlights the fact that, in order for a S-AS intensity ratio to be different from unity, two conditions are necessary: the dynamic magnetizations of the S magnons must be the complex conjugates of the AS ones (as prescribed by time reversal), and the ratio of E_x and E_y components of the radiation must be a complex number. The latter condition occurs only in an absorbing medium.

ACKNOWLEDGMENTS

One of us, R.Z., was supported by the Surfaces and Interfaces Section of INFM. F.N. acknowledges a travel grant to ANL by Consiglio Nazionale delle Ricerche. The work at ANL was supported by the U.S. Department of Energy, BES, Materials Science under Contract No. W-31-109-ENG-38. Partial financial support from MURST-COFIN 2000 is also acknowledged.

[1] R.E. Camley, Talat S. Rahman, and D.L. Mills, Phys. Rev. B **23**, 1226 (1981).

[2] R.E. Camley and M. Grimsditch, Phys. Rev. B **22**, 5420 (1980).

[3] J.F. Cochran and J.R. Dutcher, J. Appl. Phys. **64**, 6092 (1988).

[4] H. Moosmüller, J.R. Truedson, and C.E. Patton, J. Appl. Phys. **69**, 5721 (1991).

[5] J.F. Cochran, M. From, and B. Heinrich, J. Appl. Phys. **83**, 6296 (1998).

[6] R.W. Wang, D.L. Mills, E.E. Fullerton, S. Kumar, and M. Grims-

ditch, Phys. Rev. B **53**, 2627 (1996).
[7] L.D. Landau and E.M. Lifshitz, *Electrodynamics of Continuous Media* (Pergamon Press, Oxford, 1960), Chap. XIV.
[8] R.E. Camley, P. Grünberg, and C.M. Mayr, Phys. Rev. B **26**, 2609 (1982).
[9] M. Grimsditch, S. Kumar, and Eric E. Fullerton, Phys. Rev. B **54**, 3385 (1996).
[10] P.B. Johnson and R.W. Christy, Phys. Rev. B **9**, 5056 (1974).
[11] L. Giovannini, R. Zivieri, G. Gubbiotti, G. Carlotti, L. Pareti, and G. Turilli, Phys. Rev. B **63**, 104405 (2001).
[12] R. Zivieri, L. Giovannini, and F. Nizzoli, Phys. Rev. B **62**, 14 950 (2000).
[13] P. Vavassori, M. Grimsditch, E. Fullerton, L. Giovannini, R. Zivieri, and F. Nizzoli, Surf. Sci. **454-456**, 880 (2000).